

Detecting and quantifying stochastic and coherence resonances via information-theory complexity measurements

Oswaldo A. Rosso^{1,2} and Cristina Masoller³

¹*Centre for Bioinformatics, Biomarker Discovery, and Information-Based Medicine and Hunter Medical Research Institute, School of Electrical Engineering and Computer Science, The University of Newcastle, University Drive, Callaghan, New South Wales 2308, Australia*

²*Instituto de Cálculo, Facultad de Ciencias Exactas y Naturales, Universidad de Buenos Aires, Ciudad Universitaria, Buenos Aires 1428, Argentina*

³*Departament de Física i Enginyeria Nuclear, Universitat Politècnica de Catalunya, Colom 11, Terrassa, 08222 Barcelona, Spain*
(Received 12 November 2008; published 29 April 2009)

Statistical complexity measures are used to detect noise-induced order and to quantify stochastic and coherence resonances. We illustrate the method with two paradigmatic models, one of a Brownian particle in a sinusoidally modulated bistable potential, and the other, the FitzHugh-Nagumo model of excitable systems. The method can be employed for the precise detection of subtle signatures of noise-induced order in real-world complex signals.

DOI: [10.1103/PhysRevE.79.040106](https://doi.org/10.1103/PhysRevE.79.040106)

PACS number(s): 05.40.Ca, 02.50.-r, 05.45.Tp

Stochastic resonance (SR) [1] and coherence resonance (CR) [2] refer to enhanced order in a nonlinear system via an optimal amount of noise and are of major relevance in many areas of physics and biology [3–5]. For observing SR, one needs a bistable system, a noisy environment, and a sub-threshold periodic signal (i.e., a small-amplitude signal that, by itself, does not induce switchings); for observing CR, one needs an autonomous excitable system that emits noise-induced pulses or spikes; the time interval between them being the sum of an activation and an excursion time, which depend differently on the noise intensity. Optimal conditions for SR require a matching of the stochastic Kramers' escape time and the deterministic time scale of the applied signal; optimal conditions for CR, the matching of the stochastic activation, and excursion times.

The detection and the quantification of stochastic and coherence resonances can be a challenging task. SR can be quantified in terms of the intensity of a peak in the power spectrum or in terms of the intensity of several peaks in the distribution of residence times (the time intervals between consecutive switchings) [6]. The first method involves the computation of the signal-to-noise ratio (SNR), from power spectra taken at a fixed frequency of the applied signal and different noise levels; the resulting plot displaying a maximum of the SNR at a certain noise level [1]. For the second method, one computes the intensity, P_n , of the n th peak of the residence times distribution, which also displays a maximum at a certain level of noise. However, the noise levels that maximize SNR and the different peaks of the residence times distribution are not necessarily the same. Coherence resonance can be quantified by the variance of the interspike intervals (the time intervals between consecutive pulses), $R_p = \sqrt{\text{Var}(t_p)} / \langle t_p \rangle$, and by the characteristic time of the autocorrelation function [2].

It would be desirable to characterize the response of nonlinear systems to noise in terms of more subtle measures than those based on the power spectra and a probability distribution associated to the switching intervals or interspike intervals. In particular, it would be very interesting to quantify

noise-induced *temporal* order. Several statistical complexity measures have been proposed in the literature [7–9], and to the best of our knowledge, they have been overlooked for quantifying the ordering role of noise. The aim of this Rapid Communication is to show that they are suitable tools for detecting subtle signatures of noise-induced temporal order in nonlinear systems.

The statistical complexity measure is a functional that characterizes the probability distribution P associated to the time series generated by a dynamical system under study. It quantifies not only randomness but also the presence of correlational structures. The two extreme circumstances of (i) maximum foreknowledge (“perfect order”) and (ii) maximum ignorance (or maximum “randomness”) can be regarded as “trivial,” and in consequence, the statistical complexity measure must vanish for these cases. López-Ruiz, Mancini, and Calbet (LMC) [7] introduced the product functional form for a statistical complexity measure. Given a probability distribution P , associated to the state of a system, the LMC measure, is the product of the normalized Shannon entropy, $\mathcal{H}[P]$, times the disequilibrium, $\mathcal{Q}[P, P_e]$, the latter given by the Euclidean “distance” from P to P_e , the uniform distribution. Martín and co-worker [8,9] proposed a modification of the LMC measure, referred in the following as the Martín, Plastino, and Rosso (MPR) complexity, \mathcal{C} (see definition below), that consisted in the redefinition of the disequilibrium, replacing the Euclidean distance either by Wootters' statistical distance [8] or by the Jensen-Shannon divergence [9], which represent the distance between two probability distributions in the probability space Ω . It was recently shown [10] that the MPR complexity can distinguish time series generated by stochastic and by chaotic systems.

In this Rapid Communication we demonstrate that the MPR complexity measure can also detect and quantify noise-induced order. We illustrate the method with two paradigmatic nonlinear dynamical systems: a Brownian particle in a sinusoidally modulated double-well potential,

$$\frac{dx}{dt} = -\frac{\partial V(x,t)}{\partial x} + \xi(t) = x - x^3 + A \sin(\omega t) + \xi(t), \quad (1)$$

and the FitzHugh-Nagumo (FHN) model,

$$\epsilon \frac{dx}{dt} = x - \frac{x^3}{3} - y, \quad \frac{dy}{dt} = x + a + \xi(t). \quad (2)$$

In Eq. (1), $V(x,t) = -x^2/2 + x^4/4 - Ax \sin(\omega t)$. In Eq. (2), x is the activation variable, y is the slow recovery variable, and ϵ and a are constants. In both models, ξ is a Gaussian noise having zero mean, $\langle \xi(t)\xi(t') \rangle = 2D\delta(t-t')$, with D being the noise intensity.

The MPR statistical complexity can be cast as

$$\mathcal{C}[P] = \mathcal{Q}[P, P_e] \cdot \mathcal{H}[P]. \quad (3)$$

The probability distribution $P = \{p_j; j = 1, \dots, N\}$, with N being the number of possible states of the system, has associated the normalized Shannon entropy

$$\mathcal{H}[P] = S[P]/S_{\max}, \quad (4)$$

where $S[P] = -\sum_{j=1}^N p_j \ln(p_j)$ and $S_{\max} = S[P_e] = \ln N$, with $P_e = \{1/N, \dots, 1/N\}$ being the uniform distribution. Obviously, $0 \leq \mathcal{H} \leq 1$ with the limit 0 corresponding to a perfectly predictable time series (i.e., one element of P , say p_m , equals unity and the remaining p_j vanish), and 1, to a fully random one ($p_j = 1/N \forall j$).

The disequilibrium \mathcal{Q}_J is defined as [9]

$$\mathcal{Q}_J[P, P_e] = \mathcal{Q}_0 \cdot \mathcal{J}_S[P, P_e], \quad (5)$$

where \mathcal{J}_S is the Jensen-Shannon divergence,

$$\mathcal{J}_S[P_1, P_2] = \{S[(P_1 + P_2)/2] - S[P_1]/2 - S[P_2]/2\}, \quad (6)$$

and is a normalization constant, equal to the inverse of maximum possible value of $\mathcal{J}_S[P, P_e]$,

$$\mathcal{Q}_0 = -2 \left\{ \left(\frac{N+1}{N} \right) \ln(N+1) - 2 \ln(2N) + \ln N \right\}^{-1}.$$

The disequilibrium \mathcal{Q}_J reflects the systems's "architecture," being different from zero if there are "privileged" or "more likely" states among the accessible ones.

We stress the fact that the above defined statistical complexity is the product of two normalized entropies (the Shannon entropy and Jensen-Shannon divergence) but is a non-trivial function of the entropy because it depend of two different probabilities distributions, the one corresponding to the state of the system, P , and the uniform distribution, P_e . It was shown in [11] that for a given value of \mathcal{H} , there is a range of possible values for \mathcal{C} . Thus, evaluating the complexity provides additional insight in the details of a system's probability distribution, which are not described by the entropy [10,11].

A critical point is finding a suitable probability distribution, P , associated to the time series under study, $\{x_s; s=1, \dots, M\}$. This requires a partition of a D -dimensional embedding space that will, hopefully, reveal the ordinal structure of the time series [12].

Here, for defining this partition and its associated probability distribution, we use the method proposed by Bandt

and Pompe (BP) [12], which is based on a comparison of neighboring values. The BP P -generating algorithm requires that the system fulfills a weak stationary condition (for $k < D$, the probability for $x_s < x_{s+k}$ should not depend on s) [12] and that enough data is available for a correct reconstruction of the attractor.

Given an embedding dimension $D > 1$, one is interested in "ordinal patterns" of order D generated by

$$(s) \mapsto (x_{s-(D-1)}, x_{s-(D-2)}, \dots, x_{s-1}, x_s), \quad (7)$$

which assign to each time s a D -dimensional vector of values pertaining to the previous times: $s, s-1, \dots, s-(D-1)$. By the ordinal pattern related to the time (s) we mean the permutation $\pi = (r_0, r_1, \dots, r_{D-1})$ of $(0, 1, \dots, D-1)$ defined by $x_{s-r_{D-1}} \leq x_{s-r_{D-2}} \leq \dots \leq x_{s-r_1} \leq x_{s-r_0}$. In order to obtain a unique result we consider that $r_i < r_{i-1}$ if $x_{s-r_i} = x_{s-r_{i-1}}$. Thus, for all the $D!$ possible permutations π of order D , the probability distribution $P = \{p(\pi)\}$ is defined by

$$p(\pi) = \mathcal{N}\{s | s \in \mathcal{Y}; (s) \text{ has type } \pi\} / \mathcal{Y}, \quad (8)$$

where $\mathcal{Y} = M - D + 1$ and $\mathcal{N}\{\bullet\}$ stands for "number."

Because the probability distribution, P , constructed in this way takes into account the temporal structure of the time series, not only the geometrical structure of the reconstructed attractor but also *causal information*, is incorporated in the partition process that yields $P \in \Omega$ (with Ω the probability space) [13].

The selection of the embedding dimension, D , is relevant for obtaining an appropriate probability distribution because D determines not only the number of accessible states (equal to $D!$) but also the length of the time series, M , needed to have a reliable statistics (the condition $M \gg D!$ must be satisfied). For practical purposes Bandt and Pompe use $3 \leq D \leq 7$ [12]; here we use $D=6$ and analyze time series of $M=60\,000$ data points generated from numerical simulations of the bistable model [Eq. (1)] and from the FHN model [Eq. (2)]. We verified that the results are robust with respect to the value of D : similar results were found with $D=4$ and 5. For the bistable model, we analyze a sequence of M consecutive residence times; for the FHN model, a sequence of M consecutive interspike intervals.

Let us first present the results of the analysis of residence time intervals generated by the bistable system [Eq. (1)]. As discussed in the introduction, stochastic resonance occurs when the stochastic switching time scale matches the deterministic modulation time scale, and this condition can be realized by varying the noise intensity, \mathcal{D} , or the modulation frequency, ω [14]. For fixed ω , the SNR and the periodic response, $\langle x \rangle$ [1], exhibits a maximum for an optimal noise level, as shown in Fig. 1(a); however, for fixed \mathcal{D} , the resonance with the modulation frequency is not observed with these indicators, as shown in Fig. 2(a). The resonances with \mathcal{D} and with ω are both observable when plotting the amplitude of the peaks of the residence times distribution [Figs. 1(b) and 2(b)]. Let us consider the statistical complexity measures, \mathcal{C} and \mathcal{H} . It can be seen in Figs. 1(c) and 2(c) that resonantlike behavior is observed: the shape of the curves obtained is consistent with the behavior of the conventional

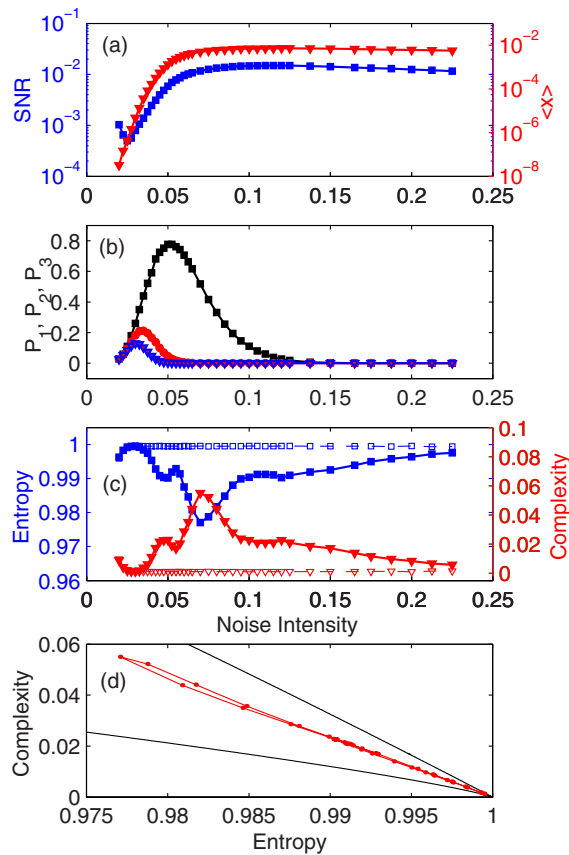


FIG. 1. (Color online) Quantifying stochastic resonance in the bistable system for varying noise intensity and fixed modulation frequency ($\omega=0.0078$). (a) The standard indicators in arbitrary units (the signal-to-noise ratio: squares; and the amplitude of the periodic component of the system response, $\langle x \rangle$: triangles) are plotted vs the noise intensity, D . (b) Amplitude of the first three peaks of the residence times distribution (P_1 : squares; P_2 : circles; and P_3 : triangles) plotted vs D . (c) MPR statistical complexity, \mathcal{C} , (filled triangles) and the normalized Shannon entropy, \mathcal{H} , (filled squares) both in arbitrary units plotted vs D . The empty symbols display \mathcal{C} and \mathcal{H} calculated using the data rearranged randomly, thus demonstrating that the statistical complexity measures \mathcal{C} and \mathcal{H} quantify temporal correlations. (d) \mathcal{C} vs \mathcal{H} (dots, red online). The solid lines indicate the boundary values, \mathcal{C}_{\max} and \mathcal{C}_{\min} .

quantifiers, SNR and $\langle x \rangle$. For instance, in Fig. 1(c) \mathcal{C} (\mathcal{H}) has a global maximum (minimum) with D , while in Fig. 2(c), \mathcal{C} (\mathcal{H}) has a tendency to decrease (increase) with ω . In both figures there are smaller local peaks that can be attributed to subtle resonantlike behavior. To further investigate this point, we analyzed the original series of residence times intervals but rearranged the data randomly. In Figs. 1(c) and 2(c) we display the results with open symbols. The resonance curves disappear, and the values for \mathcal{H} and \mathcal{C} are compatible with a pure random process ($\mathcal{H} \sim 0.999$ and $\mathcal{C} \sim 0.001$), confirming in this way that the peaked structure observed in the two information-theory quantifiers computed from the original series can be attributed to noise-induced correlations in the temporal sequence of the residence times.

The results in Figs. 1(c) and 2(c) seem to suggest that the Shannon entropy and MPR complexity measure yield the same information on the resonance; however, as explained

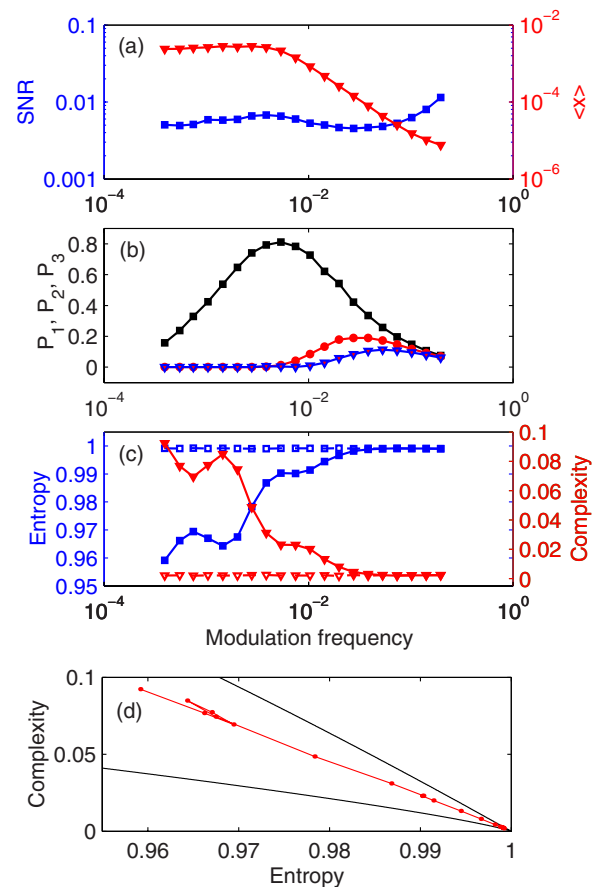


FIG. 2. (Color online) As Fig. 1, but the modulation frequency is varied while the noise level is kept fixed ($D=0.05$).

before, \mathcal{C} is a nontrivial function of \mathcal{H} , and for each value of \mathcal{H} there is a range of possible \mathcal{C} values: $\mathcal{C}_{\min} \leq \mathcal{C} \leq \mathcal{C}_{\max}$ (the procedure for calculating \mathcal{C}_{\min} and \mathcal{C}_{\max} is presented in [11]). By plotting the results in the \mathcal{C} - \mathcal{H} plane, Figs. 1(d) and 2(d), we obtain a close loop curve (that in this case is almost a line), with the left extreme being the resonance condition: maximum complexity and minimum entropy.

Figure 3 presents results of the analysis of interspike intervals generated by the excitable FitzHugh-Nagumo model [Eq. (2)]. Figure 3(a) displays the usual quantification of coherence resonance in terms of the normalized variance of interspike intervals, $R_p = \sqrt{\text{Var}(t_p)} / \langle t_p \rangle$, while Fig. 3(b) displays the MPR complexity and the normalized Shannon entropy. Here we also observe that a resonance is detected by the two introduced quantifiers. The noise level at which \mathcal{C} is maximum and \mathcal{H} is minimum is larger than that where R_p is minimum.

We interpret the above results in the following terms: since the data under investigation consist of time intervals between noise-induced switchings (for the bistable system) and between noise-induced spikes (for the FHN model), one can expect that the two quantifiers are $\mathcal{H} \approx 1$ and $\mathcal{C} \approx 0$, corresponding to a probability distribution of ordinal patterns very near to the uniform distribution [all ordinal patterns being equally probable, appearing with the same probability in the time series; see Figs. 1(c) and 2(c) with data rearranged randomly]. However, at certain noise levels, corre-

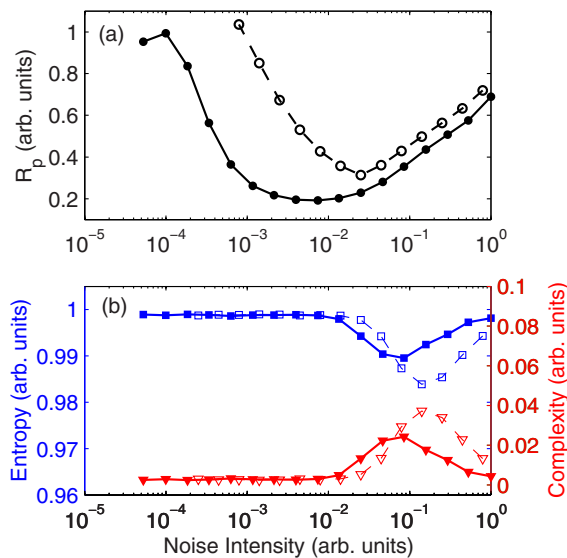


FIG. 3. (Color online) Quantifying coherence resonance in the FitzHugh-Nagumo model. (a) Normalized variance of the interspike intervals, R_p , vs the noise intensity for two sets of parameters (filled symbols: $\epsilon=0.01$ and $a=1.05$; empty symbols: $\epsilon=0.1$ and $a=1.005$). (b) MPR statistical complexity (triangles) and the normalized Shannon entropy (squares) vs the noise intensity, D , for the same parameters.

sponding to the resonances, there is an enhancement of time correlations, resulting in the probability distribution of the ordinal patterns being different from the uniform distribution. Correspondingly, there is a decrease in the entropy (revealing some degree of order) and also an increase in the sta-

tistical complexity measure. We identified this behavior as the hallmark of resonantlike behavior. We stress that similar results as those displayed in Figs. 1–3 for \mathcal{H} and \mathcal{C} were found when using embedding dimensions $D=4$ and 5. Also, when the total length of the time series was reduced to $M=30\,000$ (indicating that the probability distribution of the ordinal patterns was stationary, validating in this way the requirement $M \gg D!$).

In summary, we have shown that the information-theory measures, the normalized Shannon entropy, and MPR statistical complexity can be employed to detect and quantify resonantlike behavior in the form of enhanced temporal order induced by the variation in a system parameter or by the variation in the noise level. The success of the method is based on an appropriate reconstruction of the attractor and on an appropriate partition of the phase space that results in ordinal patterns having a probability distribution that fully characterizes the temporal correlations in the system.

Our results suggest that information-theory complexity measures can have potential for detecting subtle forms of noise-induced resonances, such as aperiodic stochastic resonance. In addition, the methodology proposed here can be used for studying the effects of heterogeneities and correlated noise in spatially extended systems [15].

O.A.R. acknowledges partial support from the Consejo Nacional de Investigaciones Científicas y Técnicas (CONICET), Argentina, and the Australian Research Council (ARC) Centre of Excellence in Bioinformatics, Australia. C.M. acknowledges partial support from the “Ramon y Cajal” Program (Spain) and the European Commission (GABA project under Project No. FP6-NEST 043309).

-
- [1] L. Gamaitoni, P. Hänggi, P. Jung, and F. Marchesoni, *Rev. Mod. Phys.* **70**, 223 (1998).
 [2] A. S. Pikovsky and J. Kurths, *Phys. Rev. Lett.* **78**, 775 (1997).
 [3] B. Lindner, J. Garcia-Ojalvo, A. Neiman, and L. Schimansky-Geier, *Phys. Rep.* **392**, 321 (2004).
 [4] G. Giacomelli, M. Giudici, S. Balle, and J. R. Tredicce, *Phys. Rev. Lett.* **84**, 3298 (2000).
 [5] R. L. Badzey and P. Mohanty, *Nature (London)* **437**, 995 (2005).
 [6] L. Gamaitoni, F. Marchesoni, E. Menichella-Saetta, and S. Santucci, *Phys. Rev. Lett.* **62**, 349 (1989).
 [7] R. López-Ruiz, H. L. Mancini, and X. Calbet, *Phys. Lett. A* **209**, 321 (1995).
 [8] M. T. Martín, A. Plastino, and O. A. Rosso, *Phys. Lett. A* **311**, 126 (2003).
 [9] P. W. Lamberti, M. T. Martín, A. Plastino, and O. A. Rosso, *Physica A* **334**, 119 (2004).
 [10] O. A. Rosso, H. A. Larrondo, M. T. Martín, A. Plastino, and M. A. Fuentes, *Phys. Rev. Lett.* **99**, 154102 (2007).
 [11] M. T. Martín, A. Plastino, and O. A. Rosso, *Physica A* **369**, 439 (2006).
 [12] C. Bandt and B. Pompe, *Phys. Rev. Lett.* **88**, 174102 (2002).
 [13] H. A. Larrondo, M. T. Martín, C. M. González, A. Plastino, and O. A. Rosso, *Phys. Lett. A* **352**, 421 (2006).
 [14] L. Gamaitoni, F. Marchesoni, and S. Santucci, *Phys. Rev. Lett.* **74**, 1052 (1995).
 [15] C. S. Zhou, J. Kurths, and B. Hu, *Phys. Rev. Lett.* **87**, 098101 (2001).